

# Statistical Analyses of Metocean Data for Offshore Wind Design in German Waters

Anja Brüning and Elimar Precht

## Summary

This paper summarises how statistical analyses of hindcast MetOcean data can be applied to find optimal solutions for offshore windfarm projects. Models can be used to generate oceanographic conditions for large sea areas where long time series can be extracted from any position of interest. The results from analysis of normal and extreme conditions are favourable informations for the design, planning and operational process of an offshore windfarm project. Based on the level of detail benefits are the development of a cost effective design and operation process as well as a better understanding of the site conditions for the development of a risk assessment for the entire lifecycle of offshore wind farms.

## Keywords

metocean data, offshore environments, extreme value analysis, probability distribution, joint probabilities

## Zusammenfassung

*Eine optimale Planung von Offshore Windparks setzt die bestmögliche Kenntnis der meteorologischen und ozeanographischen Rahmenbedingungen voraus. Dieser Artikel zeigt, wie statistische Auswertungen von Hindcastdaten zu diesem Zweck genutzt werden können. Numerische Modelle finden Anwendung, um die ozeanographischen Bedingungen großer Seegebiete zu berechnen und lange Ergebniszeitreihen an beliebigen Positionen aus der räumlichen Ergebnisdatei auszulesen. Die Ergebnisse der Analyse von Normal- und Extrembedingungen begünstigen den Entwurfs- und Planungsvorgang, sowie den betrieblichen Ablauf eines Windpark Projektes. Je nach Detailgrad kann zum Beispiel folgender Nutzen aus den Auswertungen gezogen werden: Die Entwicklung eines kosteneffektiven Entwurfs- und Betriebsplans oder eine Risikobewertung für den Lebenszyklus des Parks aufgrund eines verbesserten Verständnis der Umgebungsbedingungen.*

## Schlagwörter

*Meteorologische und hydrographische Standortbedingungen, Offshore, Extremwertanalyse, Wahrscheinlichkeitsverteilung, Multivariate Eintrittswahrscheinlichkeit*

## Contents

1	Introduction .....	168
2	Database.....	169

3	Statistical analyses of metocean data.....	170
3.1	Normal conditions.....	170
3.1.1	Time series and statistics.....	170
3.1.2	Scatter diagrams and roses.....	171
3.1.3	Fatigue data.....	172
3.1.4	Wind wave misalignment.....	173
3.1.5	Operational parameters – weather windows/persistence statistics.....	174
3.2	Extreme conditions.....	176
3.2.1	Extreme value analysis.....	177
3.2.2	On probability distributions.....	177
3.2.3	Confidence limits.....	179
3.2.4	Individual wave and crest heights.....	179
3.2.5	Short-term distributions.....	179
3.2.6	Individual Waves (Modes).....	179
3.2.7	Subset-extremes.....	181
3.2.8	Optimized subsets (directional).....	181
3.2.9	Joint Probability Analysis (JPA).....	182
4	Summary and conclusions.....	183
5	References.....	183
6	Acknowledgements.....	184

## 1 Introduction

The development of offshore wind farms requires sound and reliable meteorologic-oceanographic (MetOcean) data. Learning from the oil and gas industry and looking at available offshore standards adaptations were necessary to account for site-specific and wind farm industry related requirements. While offshore standards for structural design (DNV 2011; GL 2012; IEC 2009) provide a guideline for the methodology to be used, particular analysis tools are often subject to changes due to scientific progress and individual assessment.

Methods were established by DHI/DHI-WASY in numerous studies to provide reliable MetOcean data and related statistical parameters for design, construction/installation and O&M purposes. An overview will be given on applied statistical analyses of site-specific oceanographic parameters for normal and extreme conditions. These results can be used for the design of offshore structures with respect to either fatigue limit state (FLS), related to the possibility of failure due to the cumulative damage effect of cyclic loading, or ultimate limit state (ULS), corresponding to the limit of the load-carrying capacity.

For practical applications, preferably long time series for the project sites are evaluated. These can be derived from hindcast modelling or observational data. Methods and tools for subsequent analyses will be illustrated. Furthermore, the sensitivity to the choice of methods will be discussed. Conclusions will be drawn on the applicability and accuracy of MetOcean data for offshore design in German waters.

## 2 Database

In order to conduct statistical analysis for normal and extreme conditions within an Off-shore Windfarm (OWF) preferably long time series of water levels, currents and waves should be evaluated for the project site. These can be derived either from available measurements close to the OWF or from extracted hindcast data time series within the project area.

To date most of the OWF in the German Bight and Baltic Sea were planned in areas where observational data was not or scarcely available. Observational data sets usually cover short periods of time and may be not consistent due to time gaps. Available long time series are typically not available for the project sites proper. In most cases these data are not suitable as a base for reliable site-specific statistical analyses. A possible solution is to use the hindcast approach in order to assess the MetOcean conditions at various sites.

The hindcast approach is based on the description of large sea areas, e.g. the entire North or Baltic Sea with numerical models that are able to simulate currents and water levels as well as waves (Fig. 1). The models are driven by long time series of meteorological data. It is crucial that available observational data is used to validate the models.

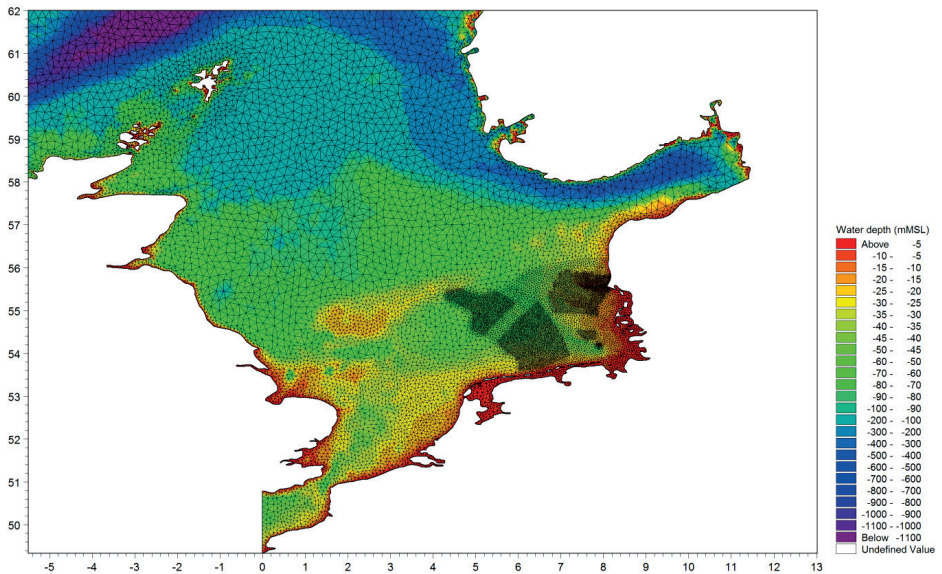


Figure 1: Bathymetry and mesh of the spectral wave model for the North Sea (focusing on the German Bight).

Modelling of currents and water levels is carried out with a hydrodynamic model, e.g. MIKE 21 HD FM (FM – flexible mesh), using long time series of astronomical tides, wind fields and atmospheric air pressure. Modelling of the waves is carried out with a last generation spectral wave model, like MIKE 21 SW FM. Boundary conditions for this model are again the wind fields and the currents and water levels from the hydrodynamic calculation, as those influence the wave field propagation and wave heights in shallow areas. Furthermore, wave spectra from a North Atlantic Model are integrated at the

model boundaries in order to account for the entering long period swell from the North Atlantic Ocean.

By means of these models it is possible to use the available long time series of wind fields to calculate waves, water levels and currents for long periods of time (hindcast). These time series can subsequently be subject to a thorough statistical analysis.

### 3 Statistical analyses of metocean data

For the design of wind turbines and their foundations, the hydrographic conditions at the location of the OWF in question are required. In order to assess the normal and extreme conditions of water levels, currents and waves, reference points for the area of interest are chosen to be analyzed. The choice depends on the size of the project area, the complexity of the bathymetry, and the level of detail required by the designer.

#### 3.1 Normal conditions

A number of analyses are carried out on observations or the established MetOcean data detailing the operational and fatigue design conditions within the project site: Time series of hourly data are evaluated statistically to provide scatter tables and plots, as well as weather windows and downtimes.

##### 3.1.1 Time series and statistics

Time series and general statistics represent the values of wind, water level, current and waves that are used for analyses of normal conditions. Parameters of interest that are directly extracted from the hindcast model are e.g. highest modelled wind speed 10 m above mean sea level ( $U_{10}$ ), the total water level range (consisting of tidal and residual – surge induced- parts), the total current speed and wave parameters, namely significant wave height ( $H_{m0}$ ), peak period ( $T_p$ ) and zero-crossing period ( $T_{02}$ ), of the total spectrum (including wind waves and swell).

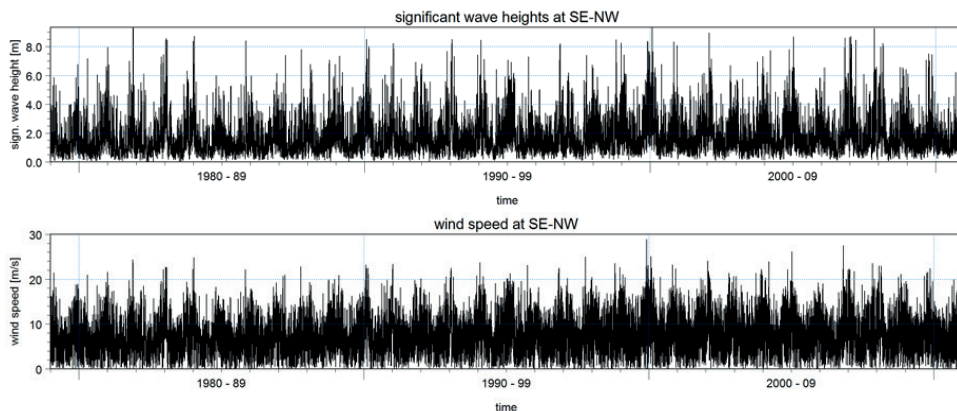


Figure 2: Long time series of modelled hindcast data for OWF Sandbank, significant wave height (top) and wind speed (bottom).

Fig. 2 exemplifies a time series of hindcast data (in this case significant wave height and wind speed at the Sandbank project site). These datasets for various parameters are the base for subsequent analyses.

### 3.1.2 Scatter diagrams and roses

Based on the metocean database, scatter diagrams/roses for the annual/omni, monthly and directional conditions can be conducted for combinations of e.g.: significant wave height vs. wave period (scatter) or wave direction (rose plot) as well as wind/current speed vs. direction. For monthly (Jan-Dec) and directional (based on MWD or  $D_{10}$ ) conditions the data base is filtered by a third parameter.

Rose plots give a good overview of the general distribution of the parameter in question. The figure for annual/omni current conditions at the project site of Sandbank presented in Fig. 3 indicates the main current directions (going to) along the NW-SE axes and shows that highest currents can be observed for the Ebb tide.

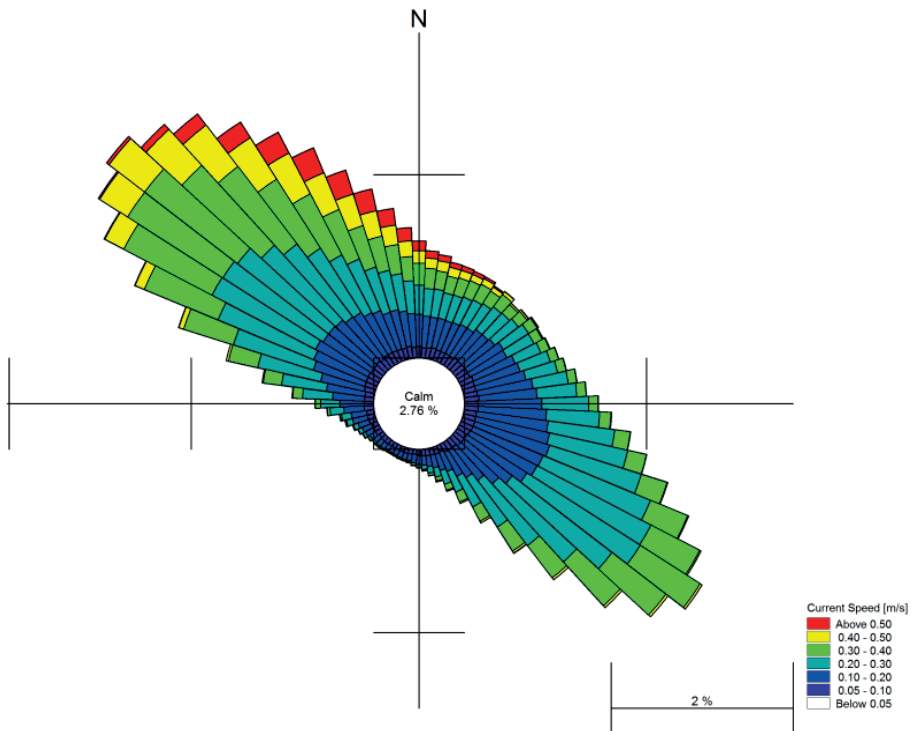
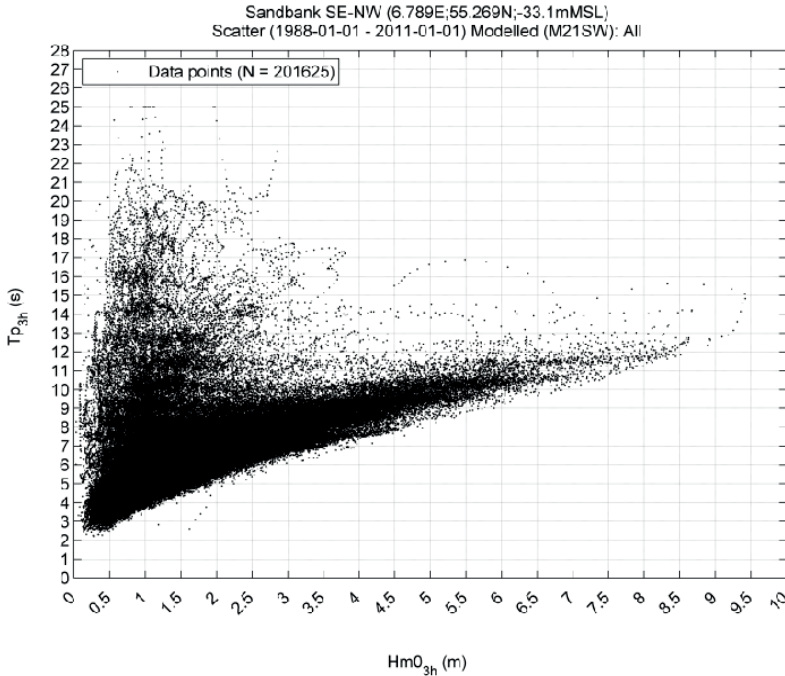


Figure 3: Current rose for Sandbank project site.

### 3.1.3 Fatigue data

For fatigue analysis, significant wave heights and their related wave periods are assessed from scatter plots and diagrams to identify the most important load cycles for e.g. the design of the foundation.

An omnidirectional scatter plot and associated diagram of significant wave height ( $H_{m0}$ ) against peak wave period ( $T_p$ ) for a 3h sea state at the Sandbank project site is presented in Fig. 4. Resolution of the scales are 1 s for  $T_p$  and 0.5 m for  $H_{m0}$ , respectively.



Reference Point Sandbank SE-NW - All Wind Directions

Sandbank SE-NW (6.789E;55.269N;-33.1mMSL)  
Absolute Occurrence: -1 (08E-C1-01 - 2011-01-31) Modelled (M21SW): All  
Hm0\_3h (m)

	[0-0.5]	[0.5-1]	[1-1.5]	[1.5-2]	[2-2.5]	[2.5-3]	[3-3.5]	[3.5-4]	[4-4.5]	[4.5-5]	[5-5.5]	[5.5-6]	[6-6.5]	[6.5-7]	[7-7.5]	[7.5-8]	[8-8.5]	[8.5-9]	[9-9.5]	[9.5-10]	Total	Accum.	
P-1	317	24	1																		344	374	
P-2	2097	1651	1116	3																		3746	8342
P-3	7472	13030	9053	416	2																	14667	35239
P-4	2781	13080	18885	5724	1189	37																31651	68481
P-5	590	3252	12024	19191	1419	3055	505	118														44211	13481
P-6	430	1318	5188	1080	1298	6013	2050	1892	207	14												15854	44238
P-7	307	759	2154	5280	2941	4469	1020	3278	1210	277	46	5										12677	37242
P-8	216	628	107	776	748	150	17	1944	2300	1808	135	185	13	6								12369	16210
P-9	107	682	140	518	291	302	194	200	355	250	187	502	208	111	37	4						3882	18112
P-10	190	460	100	371	233	120	66	156	75	32	117	120	180	126	108	36	10					3263	14527
P-11	118	306	523	420	138	82	41	27	11	12	24	38	34	7	30	26	31	16	2			1843	10700
P-12	14	277	240	206	129	52	23	14	3	3	8	18	2	5	16	4	8					1648	10466
P-13	28	311	200	133	136	60	14	13	6	4	5	2	2	9	2	2	3	2	3			1014	10620
P-14	16	247	200	82	66	31	19	4	1	3				2	1	1	1	2				859	20000
P-15	17	240	180	76	30	26	5	15						2								627	20046
P-16	3	91	180	36	10	24	10	9														359	20100
P-17	1	88	133	36	16	1																256	20134
P-18	3	91	88	26	11	1																227	20181
P-19	1	21	37	11	8	12																83	20154
P-20		2	8		2	5																13	20159
P-21		3	3																			8	20166
P-22		2	5																			5	20110
P-23		6	8	2																		15	20125
P-24																							20125
P-25																							20125
P-26																							20125
P-27																							20125
P-28																							20125
P-29																							20125
Total	81.0	4544	4748	33381	240.7	1817	18110	6388	4285	2368	150	907	622	230	133	10300	201510	77	21	9		201822	201822
Accum.	81.0	5360	6948	15477	18074	174691	104711	110101	16326	197016	16947	26414	200308	201213	201000	201510	201560	221814	221821	221822		201822	201822

Figure 4: Scatter plot and table for  $H_{m0}$  vs  $T_p$  – modelled data at OWF Sandbank.

Clear relations can be identified, this is in particular apparent during higher sea states as illustrated. However, lower sea states might include a significant fraction of longer-period waves associated with swell conditions as can be seen from the higher peak wave periods for  $H_{m0} < 4$  m in Fig. 4. Through a polynomial fit to the 1 % highest waves a correlation between significant wave height and Wave period can be derived from the data. The polynom, which describe the correlation between  $H_{m0}$  and  $T_{02}$ , or  $T_p$  respectively, is in good agreement with relationships known from literature, e.g. JOURNÉE and MASSIE 2001, WMO 1998.

Further improvements of the used hindcast models allow to use their frequency spectra for each individual sea state to determine scatter data of individual wave heights,  $H$ , vs. wave period,  $T$ , for fatigue damage calculations, instead of simply using the original time series data from the model. These scatter tables are generated by inverse Fourier transform of the modelled frequency spectra for each individual sea state, assuming a Gaussian process. Individual wave heights and wave periods are found by a zero down-crossing analysis of the generated time series of sea surface elevation. The analyses are conducted for the total part of the wave spectrum, and sea states are sorted by mean wave direction MWD.

A least-square fit of the  $H_{max}$  and  $T_{Hmax}$  mean values (based on the single maximum  $H$  in each sea state and the associated  $T$ ) is included in the applied method.

### 3.1.4 Wind wave misalignment

For wind turbine design, misalignment between the two most important dynamic forces (wind at hub height and waves) is a significant loading condition.

A scatter table between wind direction ( $D_{10}$ ) and mean wave direction (MWD) indicates the wind-wave-misalignment in total values (Fig. 5). Typically analyses are separated for different wind speeds at hub height to allow a more detailed and thus optimized design. Design optimization based on thorough analysis may lead to substantial cost savings in the design of the wind turbines.

Sandbank SE-NW (6.789E:55.269N;-33.1mMSL)  
Absolute Occurrence [-] (1988-01-01 - 2011-01-01): All  
MWD<sub>3h</sub> (°N-from)

Wind Direction (°N-from)	[15-15]	[15-45]	[45-75]	[75-105]	[105-135]	[135-165]	[165-195]	[195-225]	[225-255]	[255-285]	[285-315]	[315-345]	Total	Accum
[15-15]	2346	189	28	22	11	33	38	23	171	257	887	6566	10542	10542
[15-45]	3053	1540	122	51	23	12	9	14	97	199	509	2596	8236	18777
[45-75]	1754	2047	1792	424	113	48	18	20	118	188	387	1401	8270	28056
[75-105]	814	1134	2053	4314	2005	188	53	85	212	212	465	1122	12687	40743
[105-135]	433	348	401	1139	6578	2788	402	385	423	381	647	1418	15413	59156
[135-165]	247	124	89	193	691	4549	2520	1526	890	671	877	1030	13213	69369
[165-195]	139	36	42	85	146	785	2528	5702	2660	1316	966	890	15288	84657
[195-225]	100	29	27	22	83	161	552	8214	9719	2998	1855	1051	22648	107305
[225-255]	131	38	17	16	44	80	150	1445	12140	7898	3222	1386	26587	133872
[255-285]	142	12	9	13	18	51	75	329	3555	10628	6004	2415	24152	158024
[285-315]	222	16	4	4	16	21	38	132	714	3340	10878	7848	23239	181283
[315-345]	693	28	8	6	12	22	19	69	294	710	3914	14587	20362	201625
Total	10104	6421	4590	6271	9723	8728	6482	15953	30962	28791	31201	42369	201625	-
Accum	10104	16525	21115	27388	37109	45837	52319	68272	99284	128055	159256	201625	-	-

Figure 5: Scatter table for wind direction vs – mean wave direction at OWF Sandbank.

At present a slightly different approach is used to assess the misalignment.

The wind-wave misalignment is calculated as MWD minus  $D_{10}$  for each time step. For example, if the wind blows from south ( $WD = 180^\circ N$ ) and the waves propagate from west ( $MWD = 270^\circ N$ ), the misalignment is  $+90^\circ$ .

Scatter diagrams of the misalignment vs.  $U_{10}$  and  $H_{m0}$  and frequency distributions depict the general load incidents. For the total sea states, a significant misalignment is observed for low wind speeds (i.e. below about 10 m/s) or low  $H_{m0}$  (i.e. below 1.5 m). This is explained by the occurrence of mixed sea-states and the fact that waves propagate e.g. in the German Bight predominantly from the Northwest, while the occurrences of wind events are more evenly distributed over the directional sectors. For higher sea-states, the misalignment is reduced noticeable. The most extreme sea-states show a misalignment in the range close around  $0^\circ$ .

The sea-part of the wave spectrum is by definition fairly well correlated with the wind direction, while the swell-part of the wave spectrum shows dominating misalignment of  $-90$  and  $+90^\circ$ .

### 3.1.5 Operational parameters – weather windows/persistence statistics

Operational parameters (weather windows and downtimes) are crucial during construction and operation of OWF's. Precise datasets and thorough analyses can be used to improve the planning and optimize the operations by e.g. choosing the right time slots or vessels.

Time series of hindcast data are analysed in order to estimate the probability of occurrence of weather windows and down times for offshore works within the project site. A persistence analysis provides information regarding the long term average of weather conditions within the project area. For this purpose weather windows and downtimes for operational parameters such as significant wave height  $H_{m0}$  and wind speed  $U_{10}$  are calculated.

A weather window is defined as a period of time during which an operational condition is continuously fulfilled, this means a certain parameter is constantly below a given threshold (e.g. significant wave height  $H_{m0} < 3\text{m}$ ). The downtime period is defined as all other periods of time. Hence, the total of weather windows and downtimes for each considered weather condition corresponds to the length of the entire period of time. This definition follows the usual interpretation for logistic planning. Two different approaches, overlapping and non-overlapping can be applied when analysing weather windows.

When the non-overlapping approach is applied only total numbers of weather windows are counted. This means when a weather window beneath a parameter's threshold within a given period is counted, its number of occurrence is rounded down to an integer value instead of giving a decimal number (overlapping approach) as illustrated by Fig. 6.

Base for the analysis can be the mean value, but statistical percentiles such as the P50 (median) are used more frequently. For most of the resistant statistics the median aligns with the mean value (50 %). As long as more than half of the data do not reveal gaps, the median will lead to a correct result and a more robust statistic with regards to outliers.

The analyses can be conducted for different percentiles (e.g. P50, P75 and P90) based on a selection of thresholds for operational parameters ( $H_{m0}$ ,  $U_{10}$ ) for varying periods of time. Additionally a combination of both parameters based on their critical thresholds can be analyzed for defined durations like, e.g. 1; 3; 6; 9; 12; 18; 24; 48; and 96 hours.

The analyses are illustrated based on the P50 results at Sandbank for different thresholds of  $H_{m0}$  and duration of 12h (see Fig. 7).

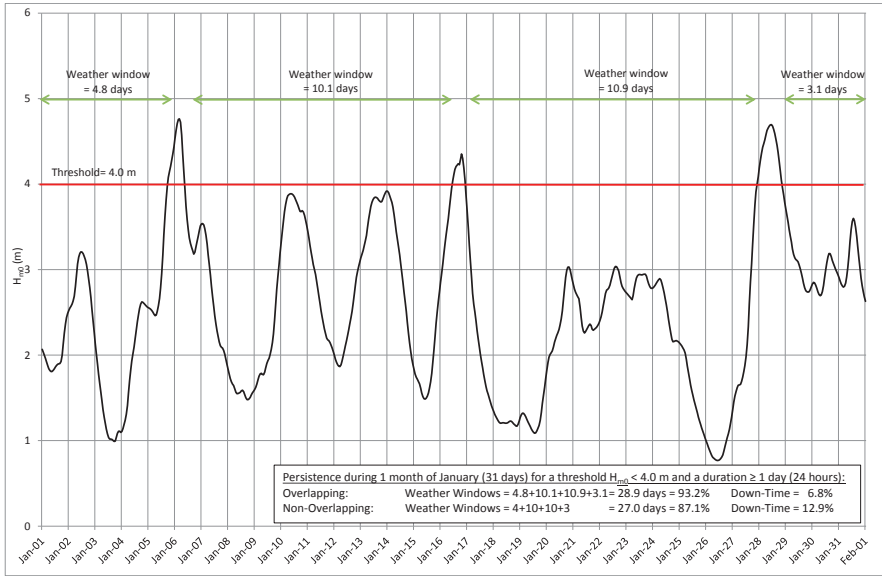


Figure 6: Weather window January (31 days) including an example for comparison between overlapping and non-overlapping methods. Both approaches refer to the definition Weather Windows + Down Times = 100%.

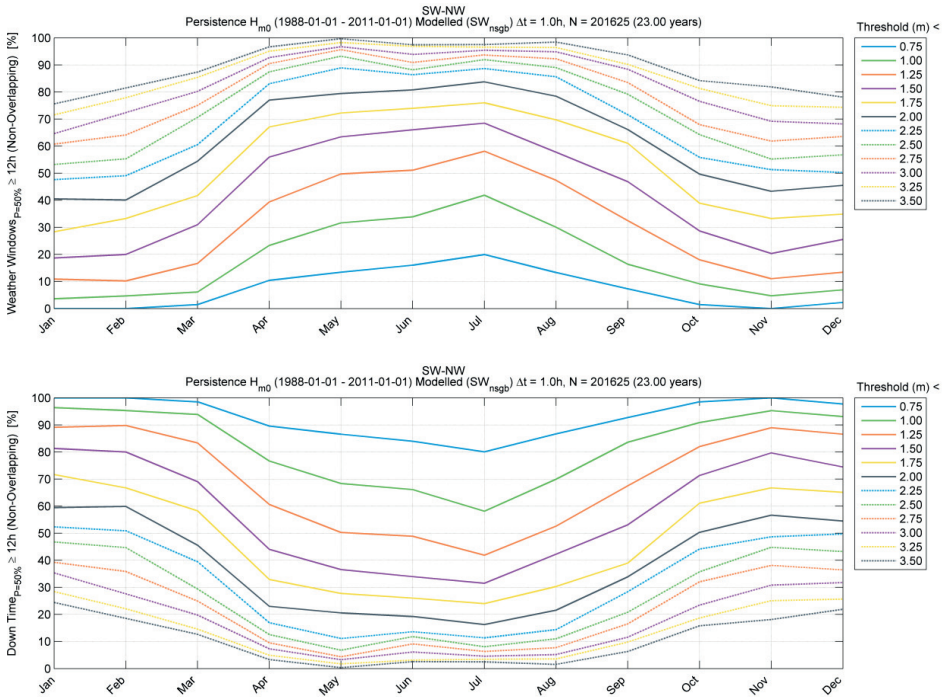


Figure 7: Diagram of weather window (top) and down time (bottom) for  $H_{m0}$  and duration of 12 h.

Seasonal results are additionally presented in Tab. 1 given as percentage of occurrence for each month. The standard deviation, which is per definition based on the mean value, is included in parenthesis to indicate the variance/scatter of each monthly bin value within a model period of 23 years.

Table 1: Table of weather window (top) and down time (bottom) for  $H_{m0}$  and duration of 12 h.

SW-NW Persistence $H_{m0}$ (1988-01-01 - 2011-01-01) Modelled ( $SW_{ns\>g}$ ) $\Delta t = 1.0h$ , $N = 201625$ (23.00 years) Weather Windows $p_{\geq 50\%} \geq 12h$ (Non-Overlapping) [%]												
	Jan	Feb	Mar	Apr	May	Jun	Jul	Aug	Sep	Oct	Nov	Dec
0.75	0.0 (1.9)	0.0 (2.9)	1.5 (4.8)	10.4 (9.9)	13.4 (10.6)	16.0 (11.2)	20.0 (13.3)	13.3 (12.2)	7.3 (5.7)	1.5 (5.1)	0.0 (3.2)	2.3 (3.1)
1.00	3.6 (6.2)	4.7 (7.4)	6.1 (10.4)	23.3 (12.2)	31.7 (13.2)	33.9 (14.8)	41.9 (16.3)	30.0 (15.3)	16.4 (9.7)	9.1 (7.7)	4.7 (7.2)	6.9 (8.0)
1.25	10.9 (11.9)	10.2 (12.1)	16.7 (12.9)	39.4 (13.1)	49.7 (12.1)	51.1 (16.4)	58.1 (16.0)	47.4 (14.7)	32.5 (11.8)	18.0 (11.0)	11.0 (12.7)	13.4 (11.2)
1.50	18.7 (14.4)	20.0 (16.8)	31.0 (15.0)	56.0 (14.8)	63.4 (10.6)	66.0 (13.9)	68.5 (14.8)	57.7 (13.7)	46.9 (14.2)	28.7 (13.7)	20.3 (15.0)	25.5 (12.2)
1.75	28.4 (15.2)	33.3 (19.0)	41.7 (16.7)	67.1 (14.3)	72.2 (9.4)	74.0 (11.4)	76.0 (13.1)	69.7 (11.2)	61.0 (14.4)	38.9 (14.5)	33.3 (16.1)	34.9 (13.4)
2.00	40.5 (18.1)	40.1 (20.9)	54.4 (17.3)	77.0 (11.4)	79.4 (7.2)	80.8 (9.5)	83.7 (10.9)	78.4 (9.2)	66.1 (13.6)	49.7 (15.7)	43.3 (16.1)	45.5 (14.8)
2.25	47.6 (18.9)	49.1 (20.6)	60.6 (18.1)	83.1 (9.2)	88.9 (5.9)	86.4 (7.3)	88.6 (9.2)	85.6 (8.0)	71.6 (12.8)	55.6 (16.3)	51.3 (15.2)	50.3 (14.7)
2.50	53.2 (19.3)	55.3 (21.3)	70.6 (18.0)	87.4 (7.5)	93.2 (4.5)	88.2 (5.9)	91.9 (7.6)	89.0 (6.6)	79.2 (11.5)	64.2 (15.9)	55.2 (14.4)	56.8 (15.5)
2.75	60.8 (19.8)	64.1 (18.5)	75.1 (17.7)	90.5 (5.8)	95.6 (3.5)	90.9 (3.8)	93.7 (5.7)	92.3 (5.8)	83.5 (10.5)	67.9 (14.9)	61.9 (13.8)	63.6 (14.4)
3.00	64.7 (19.9)	72.4 (18.1)	80.2 (16.0)	92.7 (4.9)	96.7 (2.8)	93.9 (3.5)	95.4 (4.3)	94.8 (4.3)	88.4 (9.2)	76.5 (14.6)	69.2 (12.9)	68.2 (14.1)
3.25	71.6 (19.7)	77.9 (17.1)	85.4 (14.3)	95.1 (4.3)	98.3 (2.5)	96.9 (3.0)	96.6 (3.5)	96.4 (3.1)	90.2 (7.9)	81.3 (11.5)	74.9 (12.4)	74.3 (12.6)
3.50	75.6 (19.0)	81.5 (14.8)	87.4 (12.7)	96.7 (3.5)	99.7 (1.9)	97.4 (2.6)	97.5 (2.6)	96.5 (2.8)	93.7 (6.6)	84.2 (10.8)	81.9 (10.7)	78.1 (11.6)

SW-NW Persistence $H_{m0}$ (1988-01-01 - 2011-01-01) Modelled ( $SW_{ns\>g}$ ) $\Delta t = 1.0h$ , $N = 201625$ (23.00 years) Down Time $p_{\geq 50\%} \geq 12h$ (Non-Overlapping) [%]												
	Jan	Feb	Mar	Apr	May	Jun	Jul	Aug	Sep	Oct	Nov	Dec
0.75	100.0 (1.9)	100.0 (2.9)	98.5 (4.6)	89.6 (9.9)	86.6 (10.6)	84.0 (11.2)	80.0 (13.3)	86.7 (12.2)	92.7 (5.7)	98.5 (5.1)	100.0 (3.2)	97.7 (3.1)
1.00	96.4 (6.2)	95.3 (7.4)	93.9 (10.4)	76.7 (12.2)	68.3 (13.2)	66.1 (14.8)	58.1 (16.3)	70.0 (15.3)	83.6 (9.7)	90.9 (7.7)	95.3 (7.2)	93.1 (8.0)
1.25	89.1 (11.9)	89.8 (12.1)	83.3 (12.9)	60.6 (13.1)	50.3 (12.1)	48.9 (16.4)	41.9 (16.0)	52.6 (14.7)	67.5 (11.8)	82.0 (11.0)	89.0 (12.7)	86.6 (11.2)
1.50	81.3 (14.4)	80.0 (16.8)	69.0 (15.0)	44.0 (14.8)	36.6 (10.6)	34.0 (13.9)	31.5 (14.8)	42.3 (13.7)	53.1 (14.2)	71.3 (13.7)	79.7 (15.0)	74.5 (12.2)
1.75	71.6 (15.2)	66.7 (19.0)	58.3 (16.7)	32.9 (14.3)	27.8 (9.4)	26.0 (11.4)	24.0 (13.1)	30.3 (11.2)	39.0 (14.4)	61.1 (14.5)	66.7 (16.1)	65.1 (13.4)
2.00	59.5 (18.1)	59.9 (20.9)	45.6 (17.3)	23.0 (11.4)	20.6 (7.2)	19.2 (9.5)	16.3 (10.9)	21.6 (9.2)	33.9 (13.6)	50.3 (15.7)	56.7 (16.1)	54.5 (14.8)
2.25	52.4 (18.9)	50.9 (20.6)	39.4 (18.1)	16.9 (9.2)	11.1 (5.9)	13.6 (7.3)	11.4 (9.2)	14.4 (8.0)	28.4 (12.8)	44.2 (16.3)	48.7 (15.2)	49.7 (14.7)
2.50	46.8 (19.3)	44.7 (21.3)	29.4 (18.0)	12.6 (7.5)	6.8 (4.5)	11.8 (5.9)	8.1 (7.6)	11.0 (6.6)	20.8 (11.5)	35.6 (15.9)	44.8 (14.4)	43.2 (15.5)
2.75	39.2 (19.8)	35.9 (18.5)	24.9 (17.7)	9.5 (5.8)	4.4 (3.5)	9.1 (3.8)	6.3 (5.7)	7.7 (5.8)	16.5 (10.5)	32.1 (14.9)	38.1 (13.8)	36.4 (14.4)
3.00	35.3 (19.9)	27.6 (18.1)	19.8 (16.0)	7.3 (4.9)	3.3 (2.8)	6.1 (3.5)	4.6 (4.3)	5.2 (4.3)	11.6 (9.2)	23.5 (14.6)	30.8 (12.9)	31.8 (14.1)
3.25	28.4 (19.7)	22.1 (17.1)	14.6 (14.3)	4.9 (4.3)	1.7 (2.5)	3.1 (3.0)	3.4 (3.5)	3.6 (3.1)	9.8 (7.9)	18.7 (11.5)	25.1 (12.4)	25.7 (12.6)
3.50	24.4 (19.0)	18.5 (14.8)	12.6 (12.7)	3.3 (3.5)	0.3 (1.9)	2.6 (2.6)	2.5 (2.6)	1.5 (2.8)	6.3 (6.6)	15.8 (10.8)	18.1 (10.7)	21.9 (11.6)

### 3.2 Extreme conditions

Extreme conditions of wind, wave, water levels and currents occurring at the site are determined in order to define design conditions for the ultimate limit state (ULS), corresponding to the limit of the load-carrying capacity. Precise assessment of extreme conditions is not only crucial for safety issues, a detailed and sound assessment can also be used for an optimised design which is safe and cost-efficient.

At DHI, extreme value analyses (EVA) for the parameters of interest are conducted based on sensitivity tests of a number of different distributions and thresholds, as well as fitting methods.

The assessment of individual wave heights within predefined storm sea states can be assessed based on the storm mode approach (TROMANS and VANDERSCHUREN 1995). This approach allows determining the maximum wave and/or cresting height ( $H_{max}$ ,  $C_{max}$ ) occurring during a storm based on short term distributions.

Furthermore, extreme value assessment can be constrained by monthly or directional subseries in order to account for directional or monthly variability.

### 3.2.1 Extreme value analysis

The first step in extreme value analysis is to identify the extreme events from the data, on which a probability distribution will be fitted. Various identification methods exist such as Annual Maximum Peak (AMP) or Peak Over Threshold (POT). The AMP method selects one peak per year of data, while the POT method selects all peaks above a given threshold. POT can also be referred to as the Average Annual Peak (AAP) method, if the threshold is defined by specifying an average number of peaks to be selected per year instead of a fixed threshold. The applied function and method are always very subjective depending on physical and site specific knowledge. Therefore, both AMP and AAP methods can be used in studies to perform sensitivity analyses for different distributions to find the most robust and more objective sustained estimate.

When the POT/AAP method is used, independence of the extreme events can be ensured by using an inter-event time of 36h and an inter-event level of 0.7. This means that two events can be selected as extremes only if they are separated by a minimum of 36 h and that the value ( $WS, H_{m0} \dots$ ) went below 0.7 times the peak value of the smaller of the two events. Fig. 8 depicts the POT/AAP method.

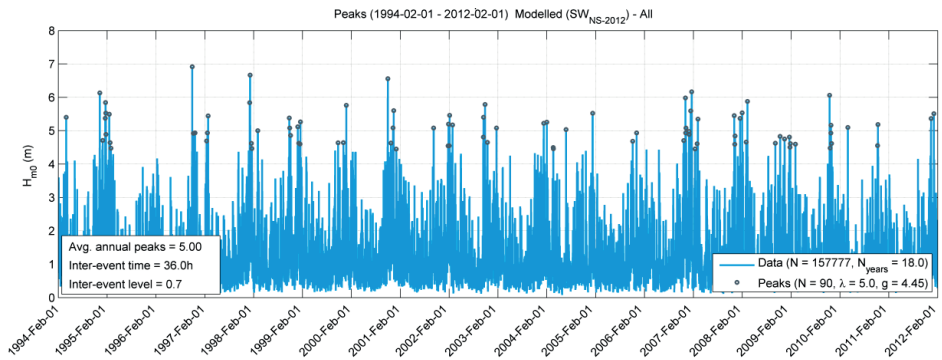


Figure 8: Time series of  $H_{m0}$  showing selected peaks using the AAP method.

### 3.2.2 On probability distributions

Extreme values with long return periods are estimated by fitting a probability distribution to historical data. A number of distributions, data selection and fitting techniques are available for estimation of extremes from historical data and the estimated extremes are often rather sensitive to the choice of method. However, it is not possible to choose a preferred method only based on its superior theoretical support or widespread acceptance within the industry. Hence, it is common practice to test a number of approaches and make the final decision based on goodness of fit. The following probability distributions are often used in connection with extreme value estimation: 2-parameter Weibull, the truncated Weibull and the Gumbel Distribution.

An example of the different fittings is given in Fig. 9 and Fig. 10 depicts an extreme distribution fit.

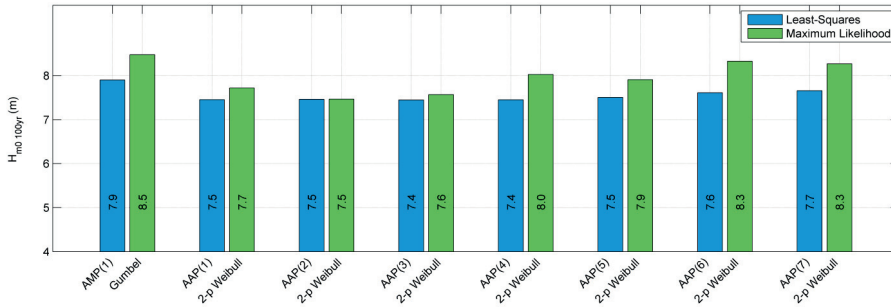


Figure 9: Omni-directional values of 100-year  $H_{m0}$  at a North Sea OWF site estimated using different distributions for a varying thresholds.

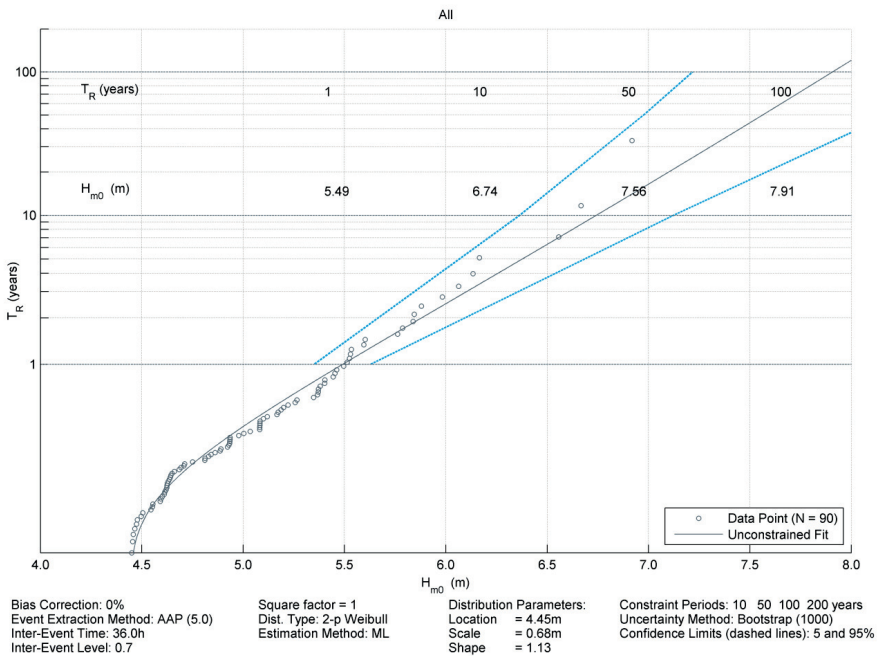


Figure 10: Extreme distribution of  $H_{m0}$  at a North Sea OWF site (UK EEZ) based on Weibull distribution (AAP = 5.0). Dots: data, black line: central estimate of extreme distribution. 5 % and 95 % confidence bounds are shown with dashed blue line.

### 3.2.3 Confidence limits

To estimate the uncertainty due to sampling errors, a bootstrap analysis is carried out on the omnidirectional extreme values. The bootstrap consists of the following steps:

- Construct a new set of extreme events by sampling randomly with replacement from the original data set of extremes
- Carry out an extreme value analysis on the new set to estimate T-year events.

An empirical distribution of the T-year event is obtained by looping step 1 and 2 many times. Quartiles are read from the empirical distribution.

The results are presented in terms of plots showing the estimated distribution and the 5 % and 95 % quartiles (dashed lines).

### 3.2.4 Individual wave and crest heights

For design purposes, the maximum wave and crest height occurring in a storm are of special interest e.g. in order to estimate the most severe ULS requiring the maximum wave height or to define the air gap at a substation based on the maximum crest height ULS. Based on hindcast data only the extreme values for significant wave heights are estimated for a certain sea state and the maximum individual wave height  $H_{\max}$  occurring in that particular storm is often derived by formulae, which does not account for the rare and rather asymptotic properties of extremes.

A more detailed approach used by DHI is to estimate the short term variability of the maximum individual wave and crest heights within a storm by using the convolution method supposed by (TROMANS and VANDERSCHUREN 1995). Here the long-term distribution of individual waves and crests is found by convolution of the long-term distribution of the modes with the short-term distribution of the maximum conditional on the mode.

### 3.2.5 Short-term distributions

The short-term distributions of individual wave heights and crests conditional on  $H_{m0}$  are assumed to follow the distributions proposed by FORRISTALL (1978 and 2000). The Forristall wave height distribution is based on Gulf of Mexico measurements, but experience from the North Sea has shown that these distributions may have a more general applicability. For this type of distribution, the distribution of the extremes of a given number of events, N, (waves or crests) converges towards the Gumbel distribution conditional on the most probable value of the extreme event,  $H_{mp}$  (or  $C_{mp}$  for crests).

### 3.2.6 Individual Waves (Modes)

The storm modes, or most probable values of the maximum wave or crest in the storm ( $H_{mp}$  or  $C_{mp}$ ), are obtained by integrating the short-term distribution of wave heights conditional on  $H_{m0}$  over the entire number of sea states making up the storm. This produces a database of historical storms each characterized by its most probable maximum individual wave height which is used for further extreme value analysis.

Peak-over-threshold estimates of the 100 year maximum wave at a North Sea OWF site are plotted as a function of the average annual number of events over threshold in Fig. 11.

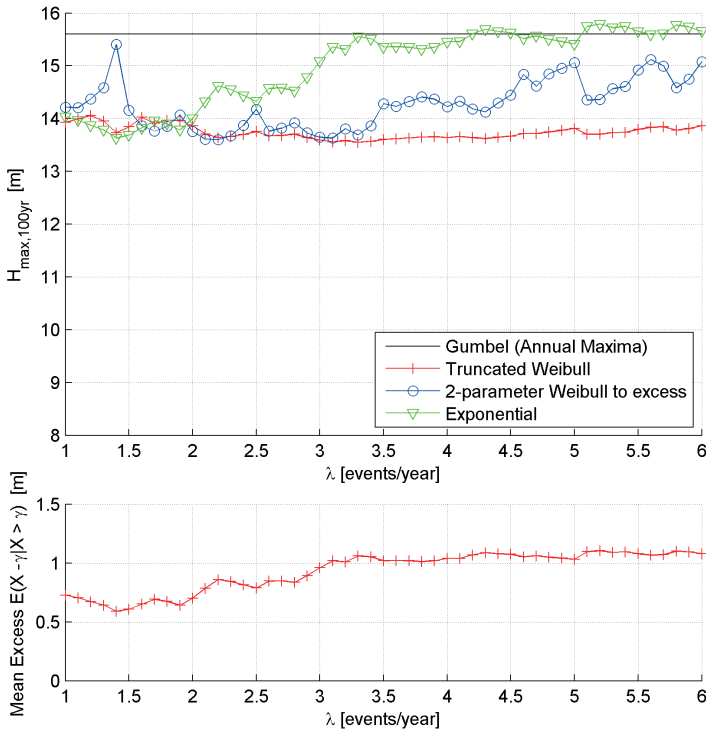


Figure 11: Omni-directional values of 100-year  $H_{max}$  at a North Sea OWF site estimated using different distributions for a varying number of selected peak events (AAP).

On-site analysis for individual crest heights follows the same approach using the short-term distribution proposed by FORRISTALL (2000). The analysis is carried out for the crest height above SWL (the instantaneous water level including effects of tide and surge).

The associated period for the maximum wave can be derived according to the recommendations in (DNV 2010) and (IEC, 2009). The stated relations are estimated for a specific area in the North Sea and therefore do not account for site specific conditions. A rather/more progressive way of estimating the relation between  $H_{max}$  and associated Period  $T_{Hmax}$  is to use the given spectral information from hindcast data. The periods associated with the maximum individual waves ( $T_{Hmax}$ ) are derived from pairs of maximum wave and associated period for each individual sea state simulation carried out to determine HT-scatter data (see Fatigue data). The joint probability model described later on is used to determine the relationship between  $H_{max}$  and its resulting median (50) periods as well as 5 and 95 percentiles (which may be used as upper and lower bounds).

### 3.2.7 Subset-extremes

Estimates of subset (e.g. directional and monthly) extremes are required for a number of parameters. These allow a better understanding of the site conditions; e.g. at a project site with highly directional extremes the developer can account for this directional extremes within the design process when e.g. boat landings or scour protection measures are planned.

In order to establish these extremes, a common practice is to fit extreme value distributions to data sampled from the modelled database that fulfil the specific requirement to direction, i.e. the extremes from each direction are extracted, and distributions fitted to each set of directional data in turn. By sampling an often relatively small number of values from the data set, each of these directional distributions is subject to uncertainty due to sampling error. This will often lead to the directional distributions being inconsistent with the omnidirectional distribution fitted to the maxima of the entire (omnidirectional) data set. Consistency between directional and omnidirectional distributions can e.g. be ensured by requiring that the product of the  $n$  directional annual non-exceedance probabilities equals the omnidirectional.

### 3.2.8 Optimized subsets (directional)

The directional extremes are derived FROM fits to each subseries data set meaning that a  $T_R$  year event from each direction will be exceeded once every  $T_R$  years on average. Having e.g. 8 directions this means that *one* of the directions will be exceeded once every  $T_R/8$  years on average. A 100-year event would thus be exceeded once every  $100/8 = 12.5$  years (on average) from *one* of the directions.

For design application, it is often required that the summed (overall) return period (probability) is  $T_R$  years. A simple way of fulfilling this would be to take the return value corresponding to the return period  $T_R$  times the number of directions, i.e. in this case the  $8 \times 100 = 800$ -year event for each direction. However, this is often not optimal since it may lead to very high estimates for the strong sectors, while the weak sectors may still be insignificant.

Therefore, an optimized set of directional extreme values is produced for design purpose in addition to the individual values of directional extremes described above. The optimized values are derived by increasing (scaling) the individual  $T_R$  values of the directions to obtain a summed (overall) probability of  $T_R$  years while ensuring that the extreme values of the strong sector(s) become as close to the overall extreme value as possible. In practice, this is done by increasing the  $T_R$  of the weak directions more than that of the strong sectors but ensuring that the sum of the inverse directional  $T_R$ 's equals the inverse of the targeted return period, i.e.:

$$\sum_{i=1}^n \frac{1}{T_{R,i}} = \frac{1}{T_{R,omni}} \quad (1)$$

where  $n$  is the number of directional sectors and  $T_{R,omni}$  is the targeted overall return period.

### 3.2.9 Joint Probability Analysis (JPA)

The probability of coincidence for two extreme parameters in question (e.g. WL and  $H_{m0}$ ) is mostly required to evaluate the unlikely event of an extreme loading condition. As an example, in the North Sea, the probability of an extreme wave occurring jointly with a very low water level is negligible, as the former are associated to westerly storms and the latter to easterly winds. Therefore it is beneficial for the design to estimate, e.g., the association between extreme high water levels and extreme wave heights to derive the probability of a joint occurrence of the two parameters.

Values of  $U_{10}$ , WL and CS associated with extremes of one variable are estimated using the methodology proposed in (HEFFERNAN and TAWN 2004). This method consists in modelling the marginal distribution of each variable separately.

No restriction is given on the marginal model of the variables. A combination of the empirical distribution for the bulk of events and a parametric extreme value distribution function fitted to the extreme tail of data has been adopted here. For parameters which may have both a positive and a negative extreme such as the water level associated to wave height, both the positive and the negative extreme tail are modelled parametrically.

Fig. 12 shows an example of the modelled dependence structure for significant wave height  $H_{m0}$  and water level  $\eta$  in physical space. The model is clearly capable of describing the positive association between wave heights and water level for this condition and appears also to capture the relatively large spreading.

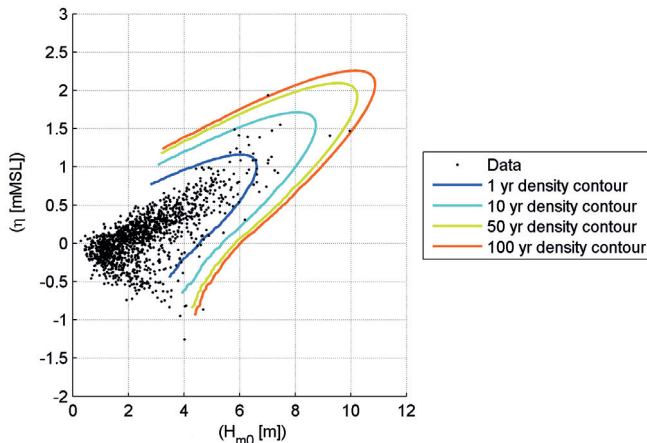


Figure 12: Dependence structure of  $H_{m0}$  and water level in physical space. Circle markers show data points and coloured lines mark the contours of constant probability density.

The applied joint probability model is event-based. This means that independent events of the conditioning parameter are extracted from the model data of hourly values. The combined inter-event time and inter-event level criterion was applied to isolate independent events of the conditioning parameter. The conditioned parameter was extracted from the model time series at the point in time of the peak of the conditioning parameter. Time averaging of the conditioned parameter is often carried out prior to data extraction in order to reduce the influence of phases in the analysis (the fact that the water level may not peak at exactly the same time as the peak wave height for instance).

## 4 Summary and conclusions

For design and operational purposes, detailed and sound knowledge of the site conditions at an OWF location are crucial for safe and cost-effective planning.

Long time series of reliable MetOcean conditions form the backbone of any sound statistical analysis. These long time series can be from measurements or from state-of-the-art numerical models that have been validated with measurements from different locations and for variable conditions.

Statistics on normal conditions give a good overview of the design-governing parameters with regards to their directional and monthly occurrence. Especially fatigue analyses based on scatter data and wind-wave-misalignment are important for the structural design. Weather statistics are a basic and most likely contractual document for the logistics planning of construction and operation of OWF's and may save costs during O&M operations as an optimised logistics approach can be chosen.

The extreme statistics presented here shows DHI's approach to determine the most severe loading conditions based on hindcast data, which are used for wind farms planned within the German EEZ waters. This ensures an optimized design including spatial and time variation of the extreme conditions as well as the joint occurrence of individual parameters.

In general the development of an offshore wind farm based on continuously improving MetOcean data and analysis will lead to a safe but not over-dimensioned and therefore cost effective construction which benefits a risk assessed planning.

## 5 References

- DHI: MIKE 21 & MIKE 3 FLOW MODEL FM Hydrodynamic and Transport Module Scientific Documentation. MIKE by DHI. Hørsholm, 2014.
- DHI: MIKE 21 Spectral Wave Module Scientific Documentation. MIKE by DHI. Hørsholm, 2014.
- DNV: Environmental Conditions and Environmental Loads, Offshore Standard DNV-RP-C205, Det Norske Veritas AS, 2010.
- DNV: Design of Offshore Wind Structures, Offshore Standard DNV-OS-J101, Det Norske Veritas AS, 2011.
- FORRISTALL, G.Z.: On the Statistical Distribution of Wave Heights in a Storm. *Journal of Geophysical Research*, Vol.83, p.2353-2358, 1978.
- FORRISTALL, G.Z.: Wave Crest Distributions: Observations and Second-Order Theory. *Journal of Physical Oceanography*, Vol.30, p.1931-1942, 2000.
- GL: Guideline for the Certification of Offshore Wind Turbines. Germanischer Lloyd, Hamburg, 2012.
- HEFFERNAN, J.E. and TAWN, J.A.: A conditional approach for multivariate extreme values. *Journal of the Royal Statistical Society*, p. 497-546, 2004.
- IEC: Design Requirements for Offshore Wind Turbines. IEC 61400-3, 2009.
- JOURNÉE, J.M.J. and MASSIE, W.W.: Offshore Hydromechanics, 1st Edition. Delft University of Technology, Maritime Technology Departement, Script. Delft, Netherlands, 2001.

- TROMANS, P. and VANDERSCHUREN, L.: Response Based Design Conditions in the North Sea: Application of a New Method, Offshore Technology Conference, Texas, USA, May 1995, OTC 7683, 1995.
- WMO: Guide to Wave Analysis and Forecasting, 2nd Edition. Secretariat of the World Meteorological Organisation, Genf, Schweiz, 1998.

## **6 Acknowledgements**

Examples from OWF Sandbank presented in this paper with kind permission from Vattenfall Europe Windkraft GmbH.